J|A|C|S COMMUNICATIONS

Published on Web 08/20/2010

Flexible Particle Array Structures by Controlling Polymer Graft Architecture

Jihoon Choi,[†] Hongchen Dong,[‡] Krzysztof Matyjaszewski,*[,‡] and Michael R. Bockstaller*[,†]

Department of Materials Science and Engineering, 5000 Forbes Avenue, and Department of Chemistry, 4400 Fifth Avenue, Carnegie Mellon University, Pittsburgh, Pennsylvania 15213

Received June 14, 2010; E-mail: bockstaller@cmu.edu; km3b@andrew.cmu.edu

Abstract: Surface-initiated atom-transfer radical polymerization is used to synthesize particle brushes with controlled fraction of extended and relaxed conformations of surface-grafted chains. In the semidilute brush limit, the grafting of polymeric ligands is shown to facilitate the formation of ordered yet plastic-compliant particle array structures in which chain entanglements give rise to fracture through a polymer-like crazing process that dramatically increases the toughness and flexibility of the particle assembly.

Current interest in the assembly of ligand-coated nanoparticles into 2D and 3D array structures is driven by the opportunities for novel material technologies that derive from the interactions within nanoparticle superlattice structures.[1] A common challenge in the solution-based assembly of particle superlattice structures is the propensity of hard-sphere-type particle assemblies to crack formation and brittle fracture during solvent evaporation.[2] Recent progress in controlled radical polymerization offers novel opportunities for polymer-stabilized colloidal systems as building blocks of particle superlattice structures.[3] Here we demonstrate that the grafting of polymeric chains can facilitate the formation of (short-range) ordered yet plastic-compliant particle array structures in which chain entanglements give rise to fracture through polymer-like crazing, thus dramatically increasing the toughness and flexibility of the particle assembly.

The particle systems in our study consist of polystyrene (PS)-grafted silica particles with average core radius $r_0 = 7.7 \pm 2$ nm with the following grafting characteristics: $\rho = 0.71$ nm^{-2}, $N = 10$, $M_w/M_n = 1.08$ (SiO_2-S10); $\rho = 0.84$ nm^{-2}, $N = 149$, $M_w/M_n = 1.21$ (SiO_2-S150); $\rho = 0.5$ nm^{-2}, $N = 773$, $M_w/M_n = 1.32$ (SiO_2-S770); and $\rho = 0.52$ nm^{-2}, $N = 1363$, $M_w/M_n = 1.79$ (SiO_2-S1360); where ρ denotes the grafting density, N the degree of polymerization, and M_w/M_n the molecular weight distribution of surface-grafted chains. Grafting of PS ligands was performed using atom-transfer radical polymerization (ATRP) as described in our previous work (see Figure 1a).[4]

Densely polymer-grafted particles (or particle brushes) are categorized depending on the polymer grafting density and degree of polymerization.[3,5] In the limit of high grafting densities, the "concentrated particle brush" (CPB) regime is observed when segmental interactions give rise to extended chain conformations.[3] As ρ decreases, a transition to the "semidilute particle brush" (SDPB) regime is observed in which reduced segmental interactions give rise to more relaxed chain conformations.[3] A generic illustration of the CPB/SDPB transition is presented in Figure 1b. Since for spherical particle brushes the effective area per chain increases

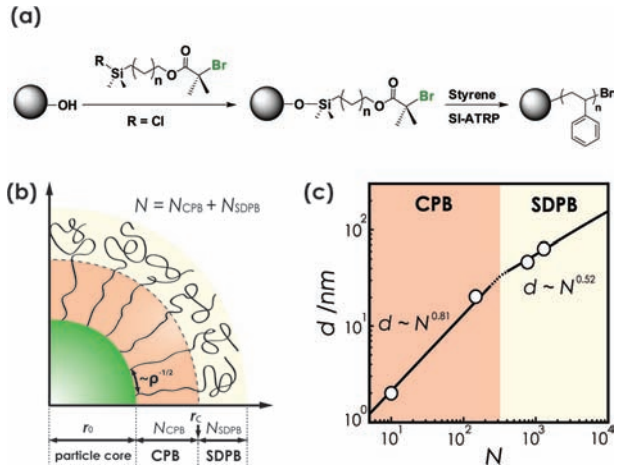

Figure 1. (a) Illustration of polystyrene grafting procedure. 1-Chlorodimethylsilylpropyl-2-bromoisobutyrate initiator is bound to the surface of silanol-functionalized silica particles. Subsequently styrene is polymerized from the surface using atom-transfer radical polymerization. (b) Illustration of "concentrated particle brush" (CPB, red) and "semidilute particle brush" (SDPB, yellow) regimes. (c) Dependence of particle surface-to-surface distance d on the degree of polymerization N of polymer grafts determined by TEM of particle monolayers (not shown). The scaling of the chain end-to-end distance $R_E \sim N^x a$ of grafted chains is $x = 0.81$ (CPB) and $x = 0.52$ (SDPB). Colored regions correspond to predicted particle brush regimes.

with increasing distance r from the particle center according to $s_{eff} = s_0(r/r_0)^2$, where r_0 denotes the particle core radius and $s_0 = 1/\rho$ the surface area per chain, a transition from the CPB to the SDPB is expected if the brush height exceeds a critical distance r_C. The latter was first proposed by Daoud and Cotton for (conceptually similar) star polymer systems as $r_C = 2\upsilon^{-1}ar_0(\pi\rho)^{1/2}$, with υ the excluded volume parameter and $a = 0.252$ nm the length of one repeat unit (here the dependence of r_C on N is neglected).[6] For the present system, the scaling of the particle surface-to-surface distance d with N of surface-grafted chains (determined by electron microscopy from particle monolayers, results not shown here) is depicted in Figure 1c, revealing that samples SiO_2-S10/S150 represent the CPB regime and samples SiO_2-S770/S1360 the SDPB regime.

In order to evaluate the effect of polymer graft modification on the cohesive properties of particle assemblies during deformation, the fracture characteristics of thin and thick particle films were elucidated using transmission electron microscopy (TEM). Thin (approximately monolayer) films were prepared by casting of dilute particle solutions ($c = 3$ mg/mL in toluene) on poly(acrylic acid) (PAA) substrate and subsequent thermal annealing in a vacuum for 24 h at $T = 120$ °C. Equilibrated films were lifted off by water immersion and transferred onto Cu grids. Cracks that formed during the film transfer were imaged by TEM using a JEOL FX2000 electron microscope. Films of 5−100 μm thickness were prepared

[†] Department of Materials Science and Engineering.
[‡] Department of Chemistry.

analogously by casting of particle solutions (c = 15 mg/mL in toluene) on PAA-coated silicon substrates.

Figure 2 summarizes the deformation characteristics of thin (panels a, c, e) and thick (panels b, d, f) particle film assemblies and reveals the transition from fragile to plastic-type deformation with increasing degree of polymerization of surface-grafted chains. In particular, for thin films of SiO_2-S10 (Figure 2a), the formation of multiple microscopic cracks is observed that are associated with macroscopic crack patterns of thick films during solvent evaporation (as shown in Figure 2b), similar to previous reports on crack formation in fragile nanocrystal superlattice structures.[2] For sample SiO_2-S150 (representing a more intermediate state between the CPB and SDPB regimes), a significantly reduced crack density was observed along with the formation of stent-like undulations across the fracture surface (Figure 2c). The scratching of supported thick films (Figure 2d) revealed wax-like characteristics similar to low-molecular-weight polymeric films. The transition to polymer-like deformation characteristics with increasing N of surface-grafted chains is most strikingly demonstrated for sample SiO_2-S770, which reveals the formation of fibrils connecting particle centers across the fracture surface during the fracture of thin films (Figure 2e) as well as the formation of flexible thick-film assemblies (Figure 2f). Analogous deformation characteristics were observed in sample SiO_2-S1360 (not shown here).

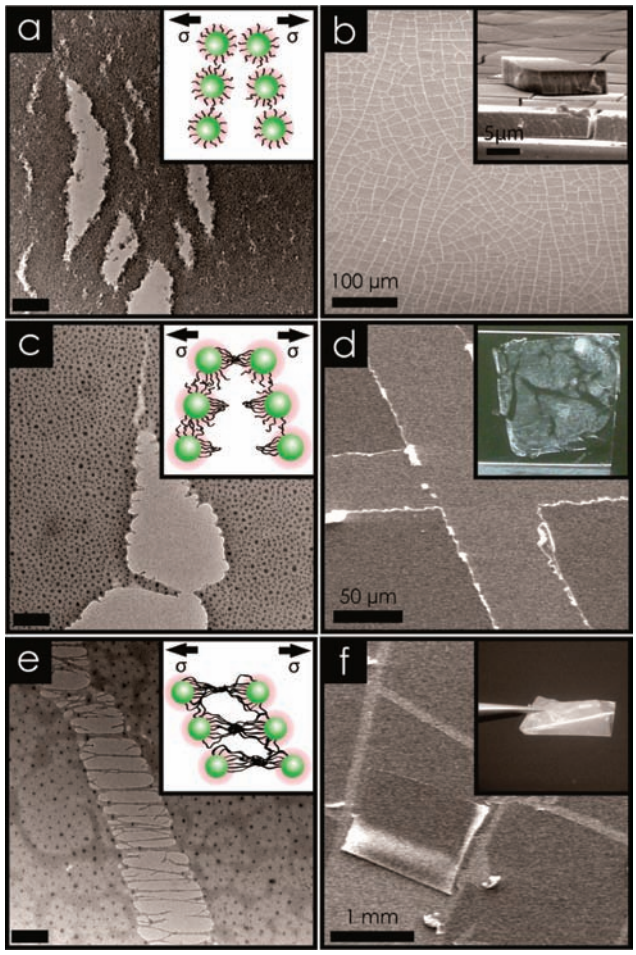

Figure 2. Deformation characteristics of particle film assemblies. (a) Bright-field transmission electron micrograph (TEM) revealing multiple crack formation in SiO_2-S10 thin (~50 nm) films. Inset illustrates crack formation normal to acting stress direction. (b) Crack pattern in SiO_2-S10 thick (~5 μm) film after solvent evaporation. Inset shows magnification. (c) Crack formation in thin (~50 nm) film of SiO_2-S10. Stent-like undulations form across the fracture surface. Inset illustrates crack formation. (d) Scanning electron micrograph (SEM) of scratched thick (~5 μm) film depicting wax-like deformation. Inset shows image of free-standing film (~50 μm) revealing fragile characteristics. (e) TEM of fracture crack in thin film of SiO_2-S770 (approximately monolayer). The formation of fibrils is observed that "bridge" particle cores across the fracture surface. Inset illustrates proposed mechanism of fibril formation by entanglement of relaxed chain segments in the SDPB regime. (f) SEM of scratched thick (~5 μm) film of SiO_2-S770, revealing peeling of film. Inset shows flexible deformation of free-standing film (~50 μm). Scale bar in panels a, c, and e is 200 nm.

The formation of fibrils in SiO_2-S770 is reminiscent to the process of craze formation in the fracture of brittle amorphous polymers (such as PS). A critical prerequisite for craze formation to occur is that the polymer molecular weight exceeds the entanglement molecular weight ($M_{crit} \cong$ 19 000 for linear PS, corresponding to N_{crit} = 183).[7] We hypothesize that the polymer-like craze formation of SiO_2-S770 originates from sufficient segments in the SDPB regime to facilitate chain entanglement. In particular, using $N = 770 = N_{CPB} + N_{SDPB}$, where N_{CPB} is determined from the definition of $r_C - r_0 = aN_{CPB}^{0.81}$, it follows that the number of segments of surface-grafted chains in the SDPB regime is $N_{SDPB} \approx 361$, thus exceeding the entanglement limit.[7] Interestingly, the analysis of micrographs such as Figure 3 reveals that the fibril extension ratio λ (defined as the maximum fibril extension L_{max} = 328.7 nm per particle surface-to-surface distance d) exceeds the maximum extension ratio of linear PS such that $\lambda \cong 1.7\ \lambda_{PS}$. Since for PS the extension ratio is, in good approximation, given as the ratio of the contour length to the equilibrium end-to-end distance of a chain segment between entanglement points (see Figure 3b), i.e. $\lambda_{PS} = l_c^e/R_E^e \sim N_e^{1/2}$, the results indicate that the effective entanglement density of particle brush systems in the SDPB regime is reduced as compared to that of linear polymer analogues, thus raising the capacity for craze extension.[7]

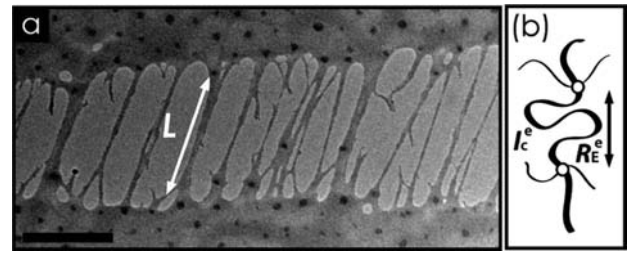

Figure 3. (a) TEM of SiO_2-S770 thin film depicting craze formation. The fibril length L is determined as the maximum (observable) length of fibrils formed between two particle centers. Scale bar is 200 nm. (b) Illustration of the structural parameters of entanglement network. R_E^e and l_c^e denote the end-to-end distance and contour length of a chain segment between entanglement points, respectively.

The synthesis of particle brush systems that are capable of forming plastic array structures with sufficient degree of order to capitalize on particle interactions could provide an important new pathway toward processable nanomaterials for a wealth of applications. The extension of the reported approach to a wider variety of graft architectures and more uniform particle systems could ultimately facilitate the tailored synthesis of particle brush systems with controlled combination of particle and polymer characteristics. Current studies focus on the relevance of particle and polymer uniformity as well as minor amounts of impurities.

Acknowledgment. Financial support by the Air Force Office for Scientific Research (via grant FA9550-09-1-0169) and The Pennsylvania Infrastructure Technology Alliance (PITA) is gratefully acknowledged.

References

(1) (a) Pileni, M. *Acc. Chem. Res.* **2008**, *41*, 1799. (b) Landman, U.; Luedtke, W. D. *Faraday Discuss.* **2004**, *125*, 1. (c) Bockstaller, M. R.; Thomas, E. L. *Phys. Rev. Lett.* **2004**, *93*, 166106.

(2) Ngo, A. T.; Richardi, J.; Pileni, M. *J. Phys. Chem. B* **2008**, *112*, 14409.

(3) (a) Ohno, K.; Morinaga, T.; Takeno, S.; Tsujii, Y.; Fukuda, T. *Macromolecules* **2007**, *40*, 9143. (b) Matyjaszewski, K.; Tsarevsky, N. V. *Nature Chem.* **2009**, *1*, 276. (c) Ojha, S.; Beppler, B.; Dong, H.; Matyjaszewski, K.; Garoff, S.; Bockstaller, M. R. *Langmuir* **2010**, *26*, 13210. (d) Matyjaszewski, K.; Xia, J. *Chem. Rev.* **2001**, *101*, 2921.

(4) Bombalski, L.; Dong, H.; Listak, J.; Matyjaszewski, K.; Bockstaller, M. R. *Adv. Mater.* **2007**, *19*, 4486.

(5) Dukes, D.; Li, Y.; Lewis, S.; Benicewicz, B.; Schadler, L.; Kumar, S. K. *Macromolecules* **2010**, *43*, 1564.

(6) (a) Daoud, M.; Cotton, J. P. *J. Phys. (Paris)* **1982**, *43*, 531. (b) D'Oliveira, J. M.; Martinho, J. M.; Xu, R.; Winnik, M. A. *Macromolecules* **1995**, *28*, 4750. (c) Voudouris, P.; Choi, J.; Dong, H.; Bockstaller, M. R.; Matyjaszewski, K.; Fytas, G. *Macromolecules* **2009**, *42*, 2721.

(7) Kramer, E. J. *Adv. Polym. Sci.* **1983**, *52*−*3*, 1.

JA105189S